Journal of Radioanalytical and Nuclear Chemistry, Vol. 269, No.3 (2006) 719–726

Chemical characterization and ^{210}Pb dating in wetland sediments from the Nhecolândia Pantanal Pond, Brazil

D. I. T. Fávaro,[1]* S. R. Damatto,[2] P. S. C. Silva,[2] A. A. Riga,[1] A. Y. Sakamoto,[3] B. P. Mazzilli[2]

[1] Centro do Reator de Pesquisas – Laboratório de Análise por Ativação Neutrônica – IPEN, Av.Prof. Lineu Prestes 2242, CEP 05508-900, São Paulo, Brasil
[2] Centro de Metrologia das Radiações – Laboratório de Radiometria Ambiental – IPEN, São Paulo, Brasil
[3] DCH/CPTL/Universidade Federal do Mato Grosso do Sul – Três Lagoas, Mato Grosso do Sul, Brasil

(Received April 6, 2006)

Pantanal, located in the central region of South America, is recognized as one of the world's largest freshwater wetlands. In order to verify possible changes in this environment, a study was undertaken in Nhecolândia Pantanal, Mato Grosso do Sul State, Brazil. Two sediment cores from the Salina do Meio pond (SM1 and SM2) and one core from a small flood land named Baía (B5) were collected in 2001. The elements As, Ba, Br, Ce, Co, Cr, Cs, Eu, Fe, Hf, La, Lu, Na, Nd, Rb, Sb, Sc, Sm, Ta, Tb, Th, U, Yb, Zn and Zr were determined by instrumental neutron activation analysis (INAA). Cluster and factorial analysis were applied to the chemical data. The sedimentation rate in the SM2 core was determined by ^{210}Pb method and the mean value found was 0.61 cm·y^{-1}. The results obtained in the present study showed that recent geochemical processes such as desorption, precipitation and dissolution can contribute for the high water alkalinity and salinity in the saline ponds.

Introduction

The immense plain of Pantanal is the world's largest freshwater wetland, a seasonally flooded plain fed by the tributaries of Paraguay River. It is located in the central region of South America (14° to 22°S and 53° to 58°E), in the Paraguay River basin, that is in the central western Brazilian states of Mato Grosso and Mato Grosso do Sul, as well as eastern Bolivia and northern Paraguay (Fig. 1). Its total area is 239,000 km^2 with 139,000 km^2 within Brazil.

Quaternary sediments, above all alluvial products of the effluents of the Paraguay River, cover this plain, which is subjected to seasonal floods, due to the hydrological regime of the main river. In the Pantanal region the landscape changes dramatically according to the two well-defined seasons of the year: the dry and the rainy ones.[1–3]

Soon after the rain starts, usually from the end of October to the end of April, the rivers overflow, not only the Paraguay River, which flows from the north through the western Pantanal, forming the border between Brazil and Bolivia and Paraguay, but also its tributaries such as the São Lourenço, Cuibá, Taquari, Miranda, Negro and Aquidauana, which flow west through the Pantanal area to the Paraguay River.

The water spreads out until the entire area is deluged to a depth of up to 3 or 4 meters except for the characteristic vegetation islands called "cordilheiras". With the flood, the depressions are inundated and form lakes known as "baías", that are generally alkaline.

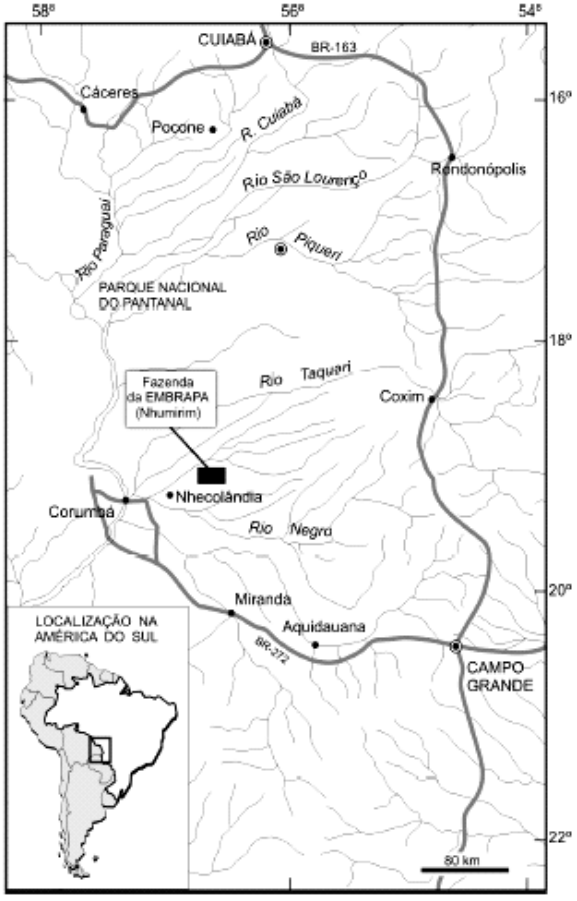

Fig. 1. Location map of the studied area from ALMEIDA et al.[15]

* E-mail: defavaro@ipen.br

0236–5731/USD 20.00

Akadémiai Kiadó, Budapest
Springer, Dordrecht

The dry period usually starts at the end of April and lasts until October. As the temperature raises, the rivers level drops. The floodwaters recede and evaporate until much of Pantanal becomes a huge grassy plain. There are still many areas where exist lakes, lagoons and saline ponds. These salinas are an essential component of the principal economical activity of this region (i.e., cattle breading). Being located in the extreme lowlands, they provide water even during the driest periods, as well as valuable mineral supplements for cattle, which feed primarily on poor-quality local grass.

Nhecolândia region, a sub-region of Pantanal, is directly influenced by the presence of the Taquari River to the west and the Negro River to the south, which presents a complex system of baías and saline ponds. These baías and saline ponds are a distinctive feature of Nhecolândia saline lakes, attributed to a past phase during the Pleistocene. However, recent studies have shown that saline and fresh water lakes are linked by a continuous water column, indicating that saline water can be originated from a contemporary concentration process.[4,5]

The area has an extremely rich and abundant variety of fauna and flora. This natural ecosystem and its biodiversity have been affected by urban contamination, irregular use of the land, uncontrolled tourism, excessive agricultural insecticide utilization, etc. The Nhecolândia ecosystem has been investigated to understand its water fluxes and solutes in waters, ground waters, soils, sediments and vegetation.

In order to verify possible changes in this environment, a study was developed in the Nhecolândia Pantanal region, Mato Grosso do Sul State, Brazil. Two sediment cores from Salina do Meio Pond and another from a small floodland named Baía were collected in 2001. The elements As, Ba, Br, Ce, Co, Cr, Cs, Eu, Fe, Hf, La, Lu, Na, Nd, Rb, Sb, Sc, Sm, Ta, Tb, Th, U, Yb, Zn and Zr were determined by instrumental neutron activation analysis (INAA). Radioactive ^{210}Pb was used to determine sedimentation rates and the sediment age of the Salina do Meio Pond.

Experimental

Two sediment cores (SM1, 59 cm long and SM2, 51 cm long) were collected in November of 2001 from Salina do Meio Pond, a depression that is situated in a low mountain range covered by arboreal vegetation. SM1 corresponds to a marginal point and SM2 to the central area of the pond, which has approximately a 70 cm water column. This salina is located in an isolated area, far from the agricultural activities and river flooding influence.

Another sediment core (81 cm long) was collected at Baía (B5). In both cases a one-inch diameter polyethylene tube was used. The cores were sliced every 2 cm resulting in 29 samples at SM1, 23 at SM2 and 41 at the B5 cores. The samples were weighed and dried at 60 °C in a ventilated oven. Then they were sifted in 0.09 mm sieves (170 mesh) with Milli-Q water and dried, and finally homogenized in a glass mortar.

The measurement of ^{226}Ra and ^{210}Pb were used to determine the dates and sedimentation rates.[6] These radionuclides were determined in each slice of the core collected at the Salina do Meio Pond (SM2). The radiochemical procedure for the determination of ^{226}Ra and ^{210}Pb was already described by MOREIRA et al.[7]

For the multielemental analysis of samples, approximately 200 mg of sediment (duplicate samples) and about 150 mg of reference materials were accurately weighed and sealed in pre-cleaned double polyethylene bags, for irradiation. Sediment samples, reference materials and synthetic standards were irradiated for 16 hours, in a thermal neutron flux of 10^{12} n·cm^{-2}·s^{-1} in the IEA-R1 nuclear reactor at IPEN. Two series of counting were made: the first, after one week decay and the second, after 15–20 days. Gamma-spectrometry was performed using a Canberra gamma X hyperpure Ge detector and associated electronics, with a resolution of 0.88 keV and 1.90 keV for ^{57}Co and ^{60}Co, respectively. The elements analyzed by using this methodology were As, Ba, Br, Co, Cr, Cs, Fe, Hf, Na, Rb, Sb, Sc, Se, Ta, Th, U, Zn, Zr and the rare earths Ce, Eu, La, Lu, Nd, Sm, Tb and Yb. The methodology validation was performed by measuring the reference materials Buffalo River Sediment (NIST SRM 2704), Soil 7 (IAEA) and BEN (Basalt –IWG-GIT).[8]

Results and discussion

The results obtained for the Buffalo River Sediment, Soil 7 and BEN reference materials analyses by INAA are presented in Fig. 2. The *Z*-value was calculated according to BODE.[9] If $|Z|<3$, the individual result of the control sample (reference material) lies in the 99% confidence interval of the target value. All *Z*-score values were in this interval ($|Z|<3$), indicating good precision and accuracy of the INAA technique.

Principal component analysis and cluster analysis (Figs 3, 4 and 5) for B5, SM2 and SM1 respectively, were applied to the results obtained for each core.

Figure 3 shows the result for cluster analysis applied to core B5 in R mode. It can be observed that the core is divided into three different groups: Group A: B5 (01-10) (0–20 cm); group B: B5 (11-25) (21–50 cm); group C: B5 (26-41) (51–81 cm). The mean value and standard deviation for each group are showed in Table 1. The mean concentration increased considerably in group C (51–81 cm) for most elements. In groups A and B, a desorption process caused by the increasing salinity, during dry season, must be the main reason for the decrease in the concentration observed for the sediment.

Under reduction conditions, iron oxy-hydroxides are dissolved releasing iron and the associated elements to the solution in pore water.[10] These elements re-precipitate in the surface layer, as the environmental condition becomes more oxidizing. In this region, this process is so effective that iron plates are formed as a result of accumulation of this element in the surface solution.[11,12]

The effect of desorption is also noted in the concentration of rare earth elements distribution with depth. The fractionation process is mainly due to systematic reduction of the ionic radius from La to Lu, which leads to the greater stability of the heavy rare earth elements (HREE) in solution and to the preferential adsorption of the light rare earth elements (LREE) on the colloidal and particulate material suspended in the waters.[13,14]

The ratio LREE/HREE (Fig. 6) decreases from top to bottom up to approximately 50 cm and increases in the deeper layers reflecting the desorption capability of HREE over LREE and its migration to the top layers.

Table 2 presents the first loading factors obtained from factorial analysis, mode R, for the three cores analyzed.

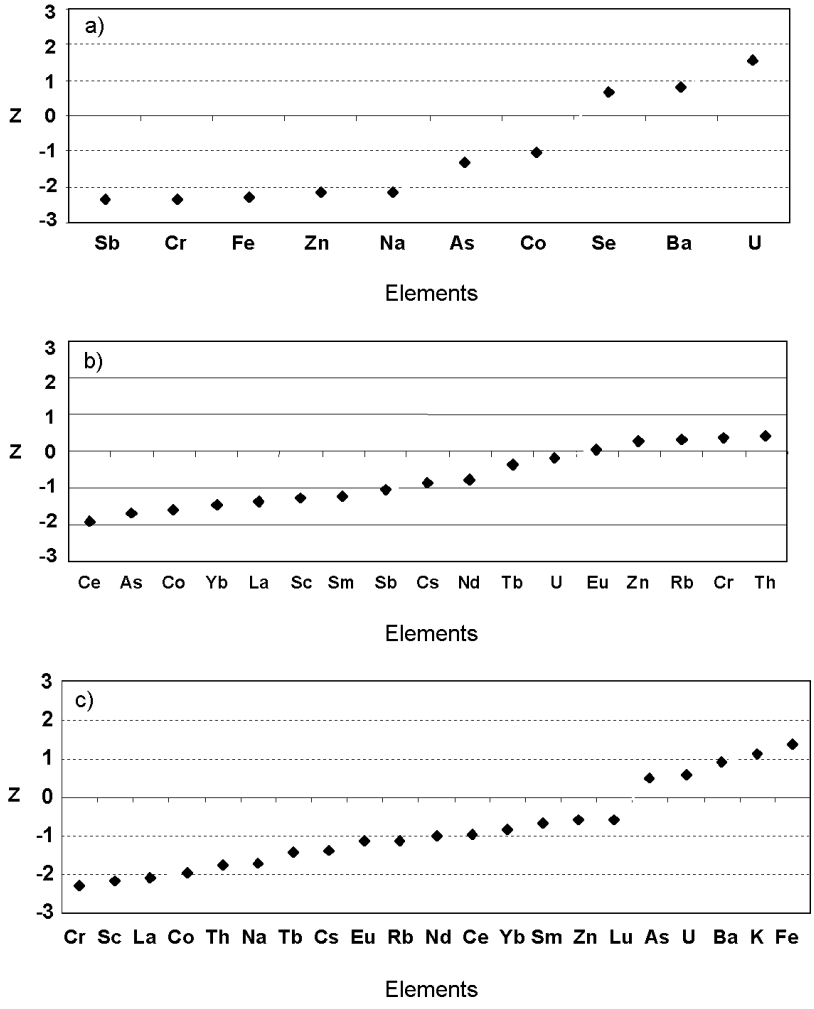

Fig. 2. Control chart (*z*-values) for inspection of the normalized concentrations of some elements in the Buffalo River Sediment NIST SRM 2704 (a), SOIL-7 (b) and BEN reference material samples (c)

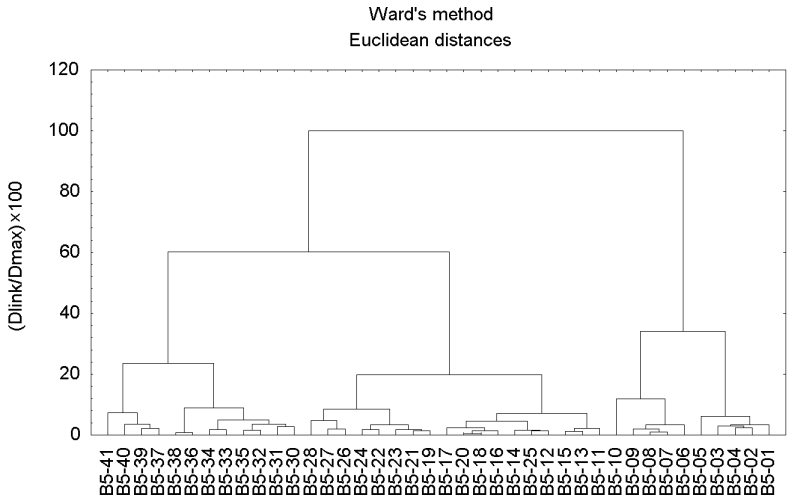

Fig. 3. Cluster analysis for the chemical data obtained from the B5 core

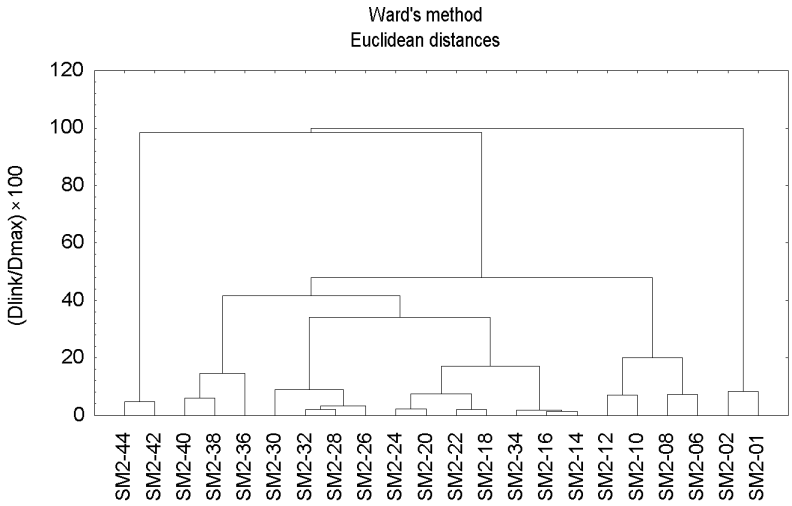

Fig. 4. Cluster analysis for the chemical data obtained from the SM2 core

Fig. 5. Cluster analysis for the chemical data obtained from the SM1 core

Table 1. Mean concentration, standard deviation (S.D.) and coefficient of variation (CV) for the groups obtained from cluster analysis

Element	B5									SM1									SM2								
	Group A			Group B			Group C			Group A			Group B			Group C			Group A			Group B			Group C		
	B5 (01-10) (0–20 cm)			B5 (11-25) (21–50 cm)			B5 (26-41) (51–81 cm)			SM1 (01-12) (0–25cm)			SM1 (13-25) (26–50 cm)			SM1 (26-29) (51–57 cm)			SM2 (01-12) (0–17 cm)			SM2 (14-34) (18–41 cm)			SM2 (36-44) (42–51 cm)		
	Mean	SD	CV	Mean	SD	CV	Mean	S.D.	CV	Mean	SD	CV	Mean	SD	CV	Mean	SD	CV	Mean	SD	CV	Mean	SD	CV	Mean	SD	CV
As	3.0	1.1	35	1.7	0.4	21	7.9	2.2	28	1.8	0.9	51	1.2	0.3	21	1.5	0.3	17	9.8	2.1	21	2.6	1.1	43	7.6	4.3	56
Ba	548	61	11	502	45	9	712	129	18	667	306	46	494	58	12	509	36	7	964	121	13	562	48	9	658	83	13
Br	2.9	2.2	75	0.4	0.2	43	0.6	0.1	27	8.8	3.2	37	12.7	2.8	22	11.4	2.0	17	11.3	6.7	59	2.6	0.4	14	3.5	0.2	6
Ce	19.2	3.2	17	22.1	3.3	15	55.3	9.7	18	14.0	4.4	32	21.7	2.4	11	29.2	2.7	9	23.9	4.2	18	34.1	13.0	38	86.9	7.0	8
Co	4.4	1.8	41	2.4	0.2	9	22.9	10.0	44	3.8	1.0	26	4.7	3.8	81	5.8	0.6	10	8.7	1.6	18	4.3	1.4	33	24.8	9.6	39
Cr	11.0	1.7	15	14.4	2.9	20	19.4	3.7	19	20.6	6.8	33	15.6	2.1	13	14.5	1.1	8	13.2	1.7	13	14.0	4.1	30	23.2	3.9	17
Cs	1.1	0.1	13	1.0	0.1	5	2.2	0.8	38	0.7	0.1	8	0.9	0.1	11	1.0	0.02	2	1.1	0.2	20	1.4	0.1	8	3.2	1.1	33
Eu	0.31	0.04	12	0.38	0.04	10	0.76	0.13	17	0.3	0.1	25	0.6	0.7	110	0.4	0.01	2	0.4	0.04	8	0.5	0.2	36	1.6	0.2	13
Fe, %	0.62	0.19	31	0.40	0.02	6	2.90	1.13	39	0.4	0.1	14	0.4	0.03	7	0.5	0.04	8	0.5	0.1	15	0.5	0.1	17	2.2	0.9	43
Hf	14.8	3.5	23	19.6	1.0	5	11.3	3.2	28	22.6	7.6	34	26.8	1.9	7	25.5	1.3	5	9.9	2.3	24	16.0	1.8	11	10.2	2.8	27
K, %	1.0	0.2	20	1.5	0.1	9	1.7	0.1	7																		
La	7.0	1.6	22	9.1	1.2	13	16.1	1.6	10	5.7	1.7	31	9.0	1.0	11	11.8	0.9	8	8.9	2.1	23	13.5	4.0	30	28.1	2.1	7
Lu	0.3	0.04	15	0.4	0.03	7	0.4	0.1	14	0.29	0.06	21	0.44	0.06	12	0.43	0.03	6	0.26	0.04	14	0.41	0.07	16	0.44	0.05	11
Na	932	213	23	1422	119	8	1445	246	17	3515	795	23	4680	336	7	5627	733	13	6409	1976	31	3244	287	9	4076	637	16
Nd	8	2	27	10	3	28	17	3	17	5.7	1.7	30	9.0	2.3	25	10.6	0.8	8	12.4	2.2	18	12.1	3.6	30	30.9	5.2	17
Rb	38	5	12	49	5	10	66	9	13	35	5	14	44	4	8	48	2	4	46	7	15	54	5	9	83	14	17
Sb	0.4	0.1	17	0.3	0.08	9	0.5	0.1	11	0.22	0.04	20	0.29	0.03	12	0.34	0.03	9	0.42	0.06	14	0.42	0.06	13	0.67	0.10	14
Sc	1.9	0.2	10	2.0	0.1	7	4.4	1.4	32	1.5	0.3	23	2.1	0.2	9	2.5	0.1	5	1.9	0.4	19	2.7	0.4	16	6.3	1.4	22
Se	0.4	0.1	30	0.6	0.2	33	0.5	0.2	48	0.9	0.1	17	0.8	0.4	49	0.7	0.1	21	0.6	0.4	67	0.7	0.2	27	0.6	0.4	62
Sm	1.3	0.3	21	1.7	0.2	13	3.0	0.8	25	1.2	0.4	32	1.6	0.4	25	2.1	0.2	9	2.0	0.6	29	2.2	1.0	45	5.6	1.2	21
Ta	0.7	0.1	13	0.9	0.1	7	0.9	0.2	23	0.8	0.3	33	1.1	0.1	10	1.2	0.1	5	0.6	0.1	24	0.9	0.4	49	1.1	0.2	20
Tb	0.2	0.1	24	0.3	0.09	14	0.5	0.1	14	0.2	0.1	32	0.29	0.04	12	0.35	0.04	11	0.3	0.1	28	0.4	0.1	22	0.8	0.1	9
Th	3.3	0.4	12	3.9	0.4	11	5.8	0.9	15	2.8	1.0	36	4.2	0.4	11	4.7	0.2	5	3.2	0.7	23	5.0	1.0	19	8.9	0.6	7
U	1.4	0.1	9	1.9	0.2	13	2.0	0.3	13	1.6	0.4	24	2.0	0.3	15	2.2	0.1	5	2.1	0.4	19	2.0	0.1	6	1.8	0.3	15
Yb	1.7	0.2	15	2.2	0.2	7	2.2	0.3	13	1.8	0.6	31	2.5	0.3	10	2.6	0.2	8	1.5	0.3	21	2.3	0.4	15	2.8	0.1	4
Zn	13	4	28	13	3	27	34	18	52	42	50	118	18	7	39	11	2	23	28	9	33	14	2	14	49	20	41
Zr	423	102	24	676	117	17	350	112	32	559	221	39	735	71	10	662	68	10	266	60	22	465	101	22	320	41	13

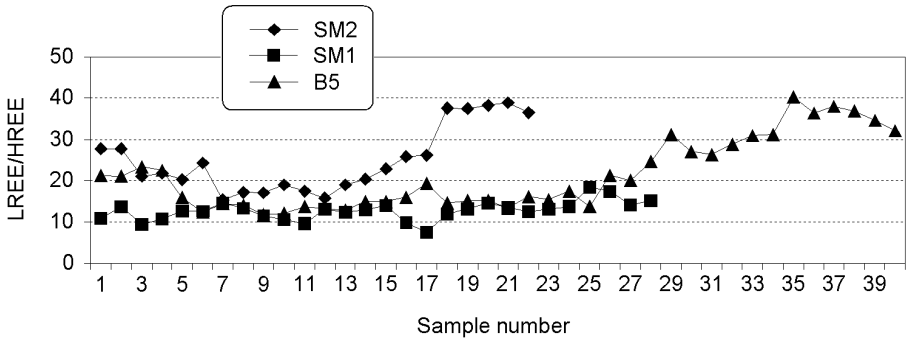

Fig. 6. LREE/HREE ratio obtained with the data from the cores B5. SM1 and SM2

From the factorial analysis, four factors were extracted in the B5 core. In factor 1, high loadings were obtained for As, Ba, Ce, Co, Eu, Fe, Hf, La, Nd, Sb and Zr; in factor 2, for Br, Lu, Na, Ta and Yb; in factor 3, for Se and in factor 4, for Cr, Cs, Sc and Zn. Factor 1 accounts for the mineralogical composition of this core sediment; while factor 2 reflects salinity variations; factor 4 reflects its granulometry, due to the presence of elements characteristics of clay minerals. These results show that granulometric variations are the factor with less influence in the variation found with depth (Fig. 3, Table 2).

Table 2. Loading factors for the first component extracted (f1) from the factorial analysis

Element	B5	SM2	SM1
As	0.94	0.23	0.05
Ba	0.90	–0.16	0.06
Br	0.10	–0.27	0.28
Ce	0.86	0.97	0.93
Co	0.91	0.87	0.18
Cr	0.44	0.87	–0.39
Cs	0.65	0.89	0.74
Eu	0.76	0.99	0.00
Fe	0.91	0.88	0.87
Hf	–0.86	–0.36	0.50
K	0.33	0.45	
La	0.75	0.95	0.93
Lu	–0.14	0.55	0.68
Na	0.16	–0.12	0.63
Nd	0.73	0.92	0.79
Rb	0.61	0.92	0.55
Sb	0.91	0.94	0.74
Sc	0.66	0.96	0.91
Se	0.17	0.15	–0.10
Sm	0.64	0.93	0.81
Ta	0.00	0.55	0.79
Tb	0.67	0.95	0.85
Th	0.61	0.93	0.86
U	0.03	–0.26	0.73
Yb	0.06	0.75	0.74
Zn	0.57	0.72	–0.19
Zr	–0.80	–0.15	0.40

Analysis for B5, SM1 and SM2 cores.

For SM2 core, cluster analysis shows three groups: group A: SM2 (01-12) (0–17 cm); group B: SM2 (14-34) (18–41 cm); group C: SM2 (36-44) (42–51 cm). The mean concentration and standard deviation for each group is showed in Table 1. From the factorial analysis, three factors were extracted. In factor 1, high loadings were obtained for Ce, Co, Cr, Cs, Eu, Fe, La, Nd, Rb, Sc, Sm, Th, Yb, and Zn; for factor 2, As, Ba, Br, Hf, Lu, Na, and Zr; and for factor 3, Sc. Factor 1 accounts for the granulometric and mineralogical composition of this core sediment samples and must be the main responsible for the distribution groups obtained in the cluster analysis (Fig. 4). For this core the same considerations made as for the B5 core are observed, that is the same variation of concentration with depth and the same pattern for the distribution of LREE/HREE ratio and iron concentration (Fig. 6). Since in this case, the water column is always present, desorption and migration processes upward sediment layers cause a decrease in the concentration in the first 41 cm. In the deeper layers, the concentration is almost constant and higher due to the decrease of water column influence. The high concentration observed for the first 4 cm reflects the re-precipitation processes caused by the increase in oxidizing conditions.

The result obtained for cluster analysis of SM1 core is showed in Fig. 5. The mean values and standard deviation obtained for the three groups formed: group A: SM1 (01-12)(0–25 cm); group B: SM1 (13-25) (26–50 cm); group C: SM1 (26-29) (51–57 cm), are presented in Table 1. Factor Analysis showed the formation of five factors. In factor 1, high loadings were obtained for Ce, Cs, Fe, La, Nd, Sb, Sc, Sm, Ta, Tb, Th, U and Yb; for factor 2, Ba, Br, and Se; for factor 3, Hf and As; for factor 4, Zn and for factor 5, Co. As can be seen in Fig. 6, this core presents a constant value for the LHREE/HREE ratio indicating that this core does not present fractionation processes affecting the rare earth distribution with depth. Although in this core the increase in concentration was not so evident with depth, this pattern was present for the elements loaded in factor 1.

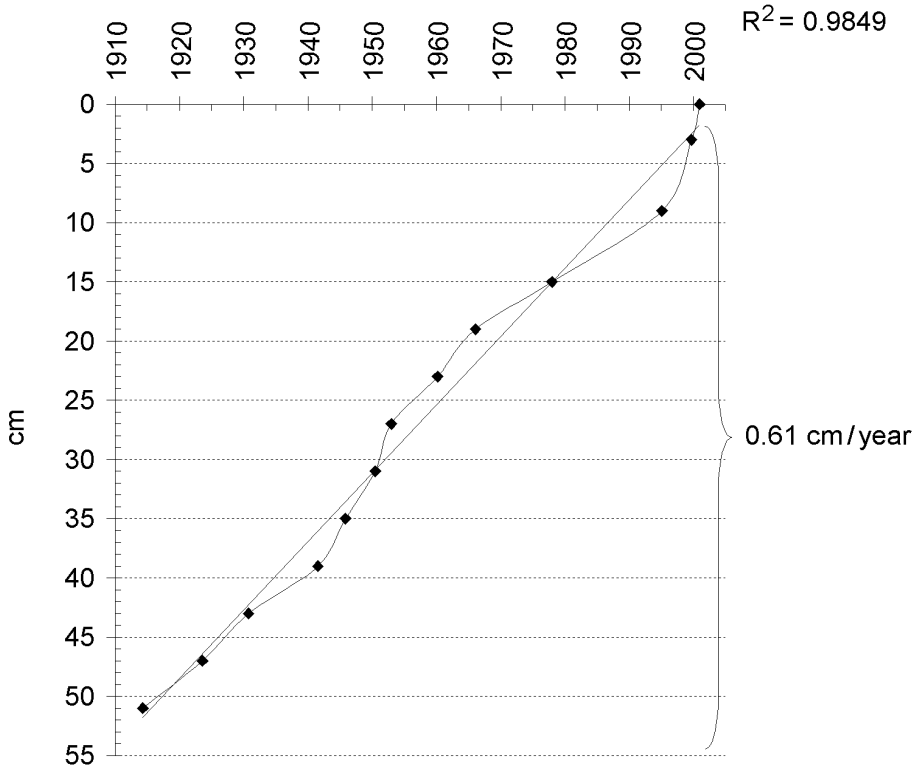

Fig. 7. Dates and sedimentation rates for sediment core SM2

According to ALMEIDA et al.,[15] the ponds protected by a stripe of dry land or "cordilheiras", covered by arboreal vegetation, are no influenced by river flooding (hydrologic control with non alkaline water afflux). During long drought periods, these ponds present higher alkalinity and salinity, occurring precipitation of organic matter and dissolved salts and the formation of bloom algae. This process is the main responsible for the increase of salinity and solute content.

Core SM2, located in the center of Salina do Meio Pond, was used for isotopic ages and sedimentation rates determination (Fig. 7). This core was selected for the calculation since it has a permanent water column. The ^{210}Pb profile depicts a well-defined linear trend from level 0 cm (year 2001) to level 57 cm (year 1914). These results indicate an average accumulation rate of 0.61 cm·y^{-1}. This accumulation rate is slightly higher than the predicted for this kind of environment,[16,17] which presents only rain and groundwater influence. The age found for the total sedimentary column analyzed (about 85 years) indicates that processes such as desorption, precipitation and dissolution play an important role in the recent geochemical conditions of the saline ponds and can contribute for the high water alkalinity and salinity.

Conclusions

The results obtained in the present study showed that recent geochemical processes such as desorption, precipitation and dissolution can contribute for the high water alkalinity and salinity in the saline ponds. The mean concentrations observed for the analyzed elements were higher in the deeper part of the cores indicating that these elements are subjected to preferential scavenge through the water column.

References

1. C. J. R. ALHO, T. E. LACHER, H. C. GONÇALVES, Bioscience, 38 (1988) 164.
2. L. BARBIÉRIO, J. P. QUEIROZ NETO, G. CIORNEI, A. Y. SAKAMOTO, B. CAPELLARI, in: III Simpósio sobre Recursos Naturais e Sócio-Econômicos do Pantanal, Os desafios do novo Milênio, Embrapa, CPAP/UFMS/Campus de Corumbá, 2000, p. 41.
3. J. P. QUEIROZ NETO, H. M. LUCATI, A. Y. SAKAMOTO, in: III Simpósio sobre Recursos Naturais e Sócio-Econômicos do Pantanal, Os desafios do novo Milênio, Embrapa, CPAP/UFMS/Campus de Corumbá, 2000.
4. L. BARBIERO, J. P. D. NETO, G. CIORNEI, A. Y. SAKAMOTO, B. CAPELLARI, E. FERNANDES, V. VALLES, Wetlands, 22 (2002) 528.

5. E. FERNANDES, A. Y. SAKAMOTO, J. P. QUEIROZ NETO, H. M. LUCATI, B. CAPELLARI, in: 4th Intern. Conf. on Geomorphology, Italy, 1997, p. 13.
6. P. G. APPLEBY, F. OLDFIELD, Catena, 5 (1978) 1.
7. S. R. D. MOREIRA, D. I. T. FÁVARO, F. CAMPAGNOLI, B. P. MAZZILLI, Environmental Radiochemical Analysis II, in: P. WARWICK (Ed.), The Royal Society of Chemistry, UK, 2003, p. 383.
8. F. E. LARIZZATTI, D. I. T. FÁVARO, S. R. D. MOREIRA, B. P. MAZZILLI, E. L. PIOVANO, J. Radioanal. Nucl. Chem., 249 (2001) 263.
9. P. BODE, PhD Thesis, Interfaculty Reactor Institute, Delft University of Technology, Delft, The Netherlands, 1996, p. 147.
10. R. B. WANTY, S. L. JOHNSON, P. H. BRIGGS, Appl. Geochem., 6 (1991) 305.
11. L. BARBIÉRIO, J. P. QUEIROZ NETO, A. Y. SAKAMOTO, in: III Simpósio sobre Recursos Naturais e Sócio-Econômicos do Pantanal, Os desafios do novo Milênio, Embrapa, CPAP/UFMS/Campus de Corumbá, 2000, p. 42.
12. A. Y. SAKAMOTO, E. FERNANDES, J. L. QUEIROZ NETO, H. M. LUCATI, B. CAPELLARI, in: VII Simpósio Brasileiro de Geografia Aplicada, Curitiba, Brasil, 1997.
13. R. H. BYRNE, K. H. KIM, Geochim. Cosmochim. Acta, 54 (1990) 2645.
14. Y. EREL, E. M. STOLPER, Geochim. Cosmochim. Acta, 57 (1993) 513.
15. T. I. R. ALMEIDA, J. B. SÍGOLO, E. FERNANDES, J. P. QUEIROZ NETO, L. BARBIERO, A. Y. SAKAMOTO, Rev. Bras. Geociências, 33 (2003) 83.
16. J. A. ROBBINS, D. N. EDGINGTON, Geochim. Cosmochim. Acta, 39 (1975) 285.
17. M. IVANOVICH, M. R. S. HARMON, Uranium-series Disequilibrium: Applications to Earth, Marine and Environmental Sciences, Clarendon Press, Oxford, 1992.